Sci. Technol. Arts Res. J., Oct.-Dec. 2023, 12(4), 52-57

DOI: https://doi.org/10.20372/star.v12i4.05

ISSN: 2226-7522 (Print) and 2305-3372 (Online)

Science, Technology and Arts Research Journal

Sci. Technol. Arts Res. J., Oct-Dec. 2023, 12(4), 52-57

Journal Homepage: https://journals.wgu.edu.et

Original Research

Analysis of impedance properties of (1-x) $Ba(Zr_{0.15}Ti_{0.85})O_3$-xCaO solid solution system

Kebede Legesse

Department of Physics, College of Natural and Computational Sciences, Wollega University, Ethiopia

Abstract

In order to differentiate between imaginary and real electrical factors, researchers employ ac impedance methods to examine material qualities. To learn about the structural and impedance properties of (1-x) Ba ($Zr_{0.15}$ $Ti_{0.85}$) O_3 - xCaO ceramics, a solid-state reaction technique was used to generate them with a composition of x=0.175. This sample was made utilizing the two-step sintering process with chemical-grade oxides and carbonate precursors (99.0-99.9%) such CaO, ZrO2, BaCO3, and TiO2. Impedance spectroscopy, an X-ray diffractometer, and the Archimedes density metre were used to characterize the synthesized samples of (1 x)Ba ($Zr_{0.15}Ti_{0.85}$) O_3 xCaO. At this specific composition, the x-ray diffraction patterns showed that the crystal structure of the (1-x) Ba ($Zr_{0.15}Ti_{0.85}$)O_3 - xCaO exhibited tetragonal symmetry, with a lattice constant of 6.12A˛ and a c-value of 7.23A˚. At a steady temperature, the actual impedance drops dramatically with frequency until it shows no change at all as the frequency increases. At 180439.55 Hz, the imaginary impedance peaks. Based on the combined analysis of structural, density, and impedance properties, the (1-x) Ba($Zr_{0.15}Ti_{0.85}$)O_3-xCaO solid solution system is expected to be a new candidate electro ceramic material, according to important facts about the system.

Article Information

Article History:

Received : 02-10-2023

Revised : 30-11-2023

Accepted : 27-12-2023

Keywords:

Structure, Impedance property, Barium zirconium titanate, calcium oxide.

*Corresponding Author:

Kebede Legesse

E-mail:

kebedelegesse@gmail.com

INTRODUCTION

There has been extensive research on the generic formula for perovskites, ABX3, in recent years. Here, X represents the oxygen ion O2−. The cation sites of perovskite oxides are frequently A or B partly substituted, and they have high oxygen mobility. According to Siqueira et al. (2023), the charge carrier, which might be an electron or a hole, causes electrical conductivity, whereas the O2− anion causes ionic conductivity. The ABO_3 type of perovskite oxides is one variant of these materials; they have a standard perovskite structure with several elements occupying the A and B sites. Perovskite oxides have a wide range of applications, including energy storage, transducers, quantum electromagnets, spintronic devices, and multistate memory devices (Dabas et al., 2020; Das et al., 2008). reduced by xThe perovskites substance *$Ba(Zr_{0.15}Ti_{0.85})O_3$-xCaO* contains several elements at its A and B sites. An electrical circuit's impedance is defined as the sum of its reactance and resistance, as stated by Ahmad et al. (2014). The many electrical conduction

phenomena in solid crystalline materials are mostly dictated by the crystal structure. Hoping of mobile charges (electrons, holes, and polarons) is a topic of great importance in charge conduction. Impedance spectroscopy (IS) is a relatively new and powerful method for determining the conduction process, defining extensive electrical properties, and studying interactions with electrically conducting electrodes in a material. Any solid material, such as an ionic, semiconducting, mixed electronic-ionic, or even an insulator (dielectric)—charge dynamics in bulk and interfacial regions can be studied using this method (Roy et al., 2013). The capacity to assess a material's potential for usage in numerous innovative contexts is aided by knowledge of its electrical conductivity. According to Ahmad et al. (2014) and Roy et al. (2013), the properties of *(1-x) $Ba(Zr_{0.15}Ti_{0.85})O_3$-xCaO* can be changed by adjusting the sintering process, the kind and amount of additives, and the circumstances and method of preparation. Because different cations cause different changes in the host lattice, improving the electrical and structural properties of *(1-x) $Ba(Zr_{0.15}Ti_{0.85})O_3$-xCaO* is thus achievable by careful cation selection. Important for the measured electrical behaviors, the mobility of the charge carriers is induced by the distribution of cations between the A- and B-sites (Primo et al., 2001). The use of Ca2+ ions as nonmagnetic sample additions is of interest to several investigations, among which are those involving the various divalent cations (Thakur et al., 2016). The impedance characteristics and structural analysis of a calcium-doped barium zirconium titanate (Ba($Zr_{0.15}Ti_{0.85}$)) sample were investigated using a composition with x = 0.175. Researchers expected composites composed of these ceramics to have the benefits of both systems. This prompted a comprehensive investigation into the electrical and structural properties of *(1-x)$Ba(Zr_{0.15}Ti_{0.85})O_3$-xCaO* ceramics with x = 0.175.

MATERIALS AND METHODS

Nanocrystalline

To make the *(1-x)$Ba(Zr_{0.15}Ti_{0.85})O_3$-xCaO* samples (where x = 0.175), the high-temperature solid-state reaction process used CaO, ZrO_2, $BaCO_3$, and TiO_2 as starting ingredients. Acetone (C3H6O2) and polyvinyl alcohol powder (C_2H_4O) were also used. All starting powders were extremely pure to avoid detrimental effects on sample quality caused by uncontrolled chemical reactions that could have occurred during preparation. oxides and carbonates of chemical grade (99.0–99.9%) utilized as building blocks initially. The precursors were usually used in stoichiometric amounts in the synthesis techniques. Afterwards, the powder that was produced was compacted into pellets with dimensions of around 1.5 mm thick and 6.7 mm in diameter. After that, it was heated to 700 °C and 950 °C for a full day. The XRD and impedance analyzer were used to characterize the sample device. The structure, impedance properties, density, and crystallite size of the sample material were all determined using these equipment.

RESULTS AND DISCUSSION

The crystalline structures of solids are fundamental for depicting their general properties and determining the many physical

features that differentiate them from other materials. Figure 1 below shows the XRD patterns for the *(1-x)Ba($Zr_{0.15}Ti_{0.85}$)O_3-xCaO* samples, and Table 1 includes some associated results. This is because there is a significant link between the structural properties and the impedance properties of (*(1-x) Ba ($Zr_{0.15}Ti_{0.85}$) O_3-xCaO*. The structural features of the synthesized powders with the composition (*(1-x)Ba($Zr_{0.15}Ti_{0.85}$)O_3-xCaO* (x = 0.175) were examined using an at-room temperature operational X-ray diffractometer.

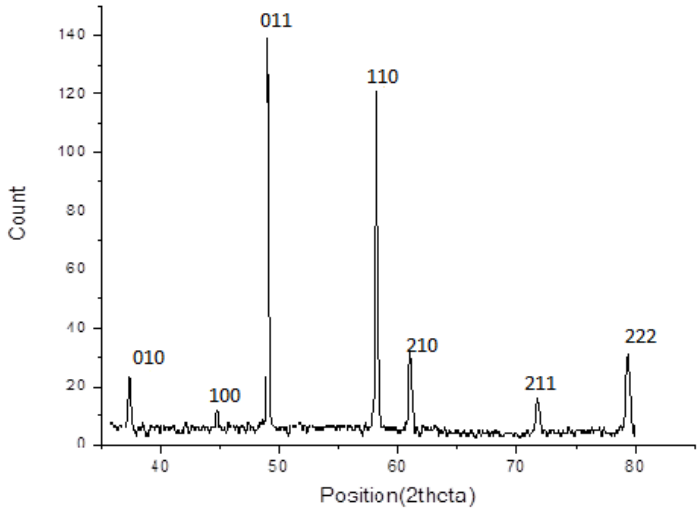

Figure1. *XRD pattern of (1-x)Ba($Zr_{0.15}Ti_{0.85}$)O_3-xCaO ceramics*

The XRD pattern of the powder ceramics (*(1-x)Ba($Zr_{0.15}Ti_{0.85}$)O_3-xCaO* is shown in Figure 1, following sintering at 950˚C and calcination at 700˚C. A single-phase perovskite structure has developed in the sample, according to an analysis of the *(1-x)Ba($Zr_{0.15}Ti_{0.85}$)O_3-xCaO* ceramics XRD pattern. Additionally, following sintering, the data clearly demonstrate the absence of diffraction peaks originating from impurity phases. According to Alaeddin et al. (2010), this means that Ca can diffuse into the *Ba($Zr_{0.15}Ti_{0.85}$)O_3* lattice structure and create solid solutions. Since there was no sign of any extra peaks caused by the oxides that made up the compound, and the computed and observed inter-planar spacing were in excellent agreement, it was likely that a single-phase complex had been formed. The compound *(1-x)Ba($Zr_{0.15}Ti_{0.85}$)O_3-xCaO*, where x = 0.175, displays distorted cubic structure development, suggesting the presence of additional structures rather than the cubic structure. The tolerance factor for this phenomenon is 1.11. The reflection pattern indicates the presence of tetragonal phases with edge lengths of 6.12A˚ and 7.23A˚, respectively. It must be remembered that ceramic materials' dielectric characteristics can be affected by their densification and composition (Bashir et al., 2011). According to Table 1, the relative density in this study ranges from 82.50% to 92.50%. The shift in impedance characteristics may be due in large part to this. Debye Scherer's formula and XRD tests yielded a crystallite size of 19.14 nm.

Table 1

Structure, crystallite size and density of (1-x) Ba ($Zr_{0.15}Ti_{0.85}$)O_3-xCaO ceramic

Composition	Structure	Lattice Parameters (A°)	Relative Density (%)	Porosity %	Crystallite size (nm)	Tolerance factor
0.175	tetragonal structure	a = 6.12 c = 7.23	92.50	7.50 %	19.14	1.11

Impedance analysis

Impedance analysis is a powerful tool for studying the electrical and dielectric properties of a material. Z* = Z′ + iZ″ is the formula for the impedance of the materials. where the real part of the impedance is Z′ and the imaginary part is Z″. Observed in Figure 2, the actual impedance component (Z′) varies with frequency.

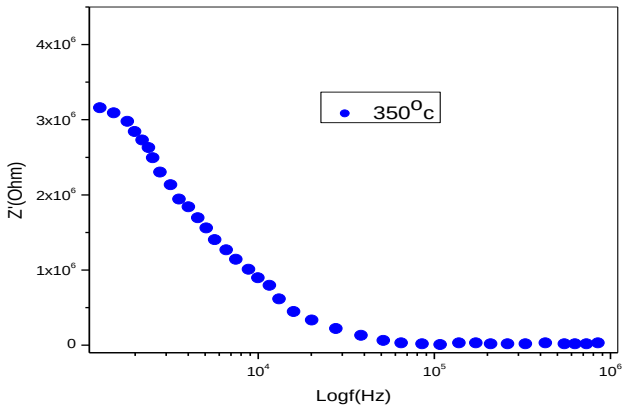

Figure2. *Z′ versus frequency plot at constant temperature*

An increase in ac conductivity and a negative temperature coefficient of resistance (NTCR) are shown by the fact that Z′ decreases with increasing frequency at constant temperature (Jonscher, 1977). Z′ is higher in the low-frequency region due to charge buildup at grain boundaries, and it becomes frequency-independent in the high-frequency zone. According to Deka et al. (2017), this high-frequency behavior is caused by the release of space charges. With less time to relax, space charge recombination would happen faster at higher frequencies. The graph clearly shows that Z' decreases with increasing frequency. As the frequency increases, the real impedance (Z') often drops until it shows no change at all.

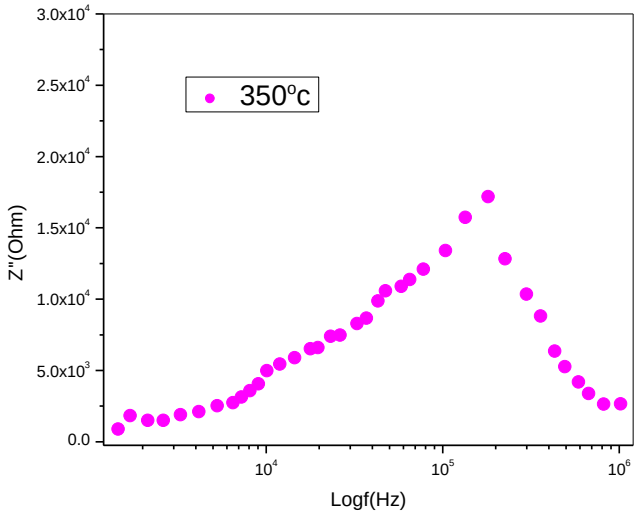

Figure3. *Z″ versus frequency plot at a constant temperature*

Figure 3 shows the relationship between frequency and the imaginary part of the impedance (Z″) at a constant temperature. In the *(1-x)Ba($Zr_{0.15}Ti_{0.85}$)O_3-xCaO* ceramic, the Z" frequency dependency reaches its maximum at 350 °C, as shown in the figure. At a frequency of 180439.55Hz, the imaginary impedance achieves its minimum and practically remains constant, whereas Z″ reaches its maximum at Z", according to the graph.

CONCLUSION

We used a solid-state reaction technique at high temperature to synthesize the polycrystalline sample *(1-x)Ba($Zr_{0.15}Ti_{0.85}$)O_3-xCaO*. At constant temperature, the impedance structure and behavior of the (*(1-x)Ba($Zr_{0.15}Ti_{0.85}$)O_3-xCaO* sample were studied in great detail. The XRD reflection pattern of this substance shows that it has a tetragonal structure. This investigation confirms that the imaginary and real impedances are field dependent. The peak heights tend to drop off as the frequency goes up. Eventually, they merge in the HF band. This demonstrates that space charge polarisation is detectable at low frequencies but disappears at high ones. The combined structural and impedance analysis clearly indicates that this material has potential applications in electro-ceramic materials.

ACKNOWLEDGMENTS

The author would like to thank Wollega University for funding for the research work.

DECLARATION

The author declares that there is no conflict of interest.

DATA AVAILABILITY STATEMENT

All data are available from the corresponding author upon request.

REFERENCES

Ahmad, I., Akhtar, M. J., & Hasan, M. M. (2014). Impedance spectroscopic investigation of electro active regions, conduction mechanism and origin of colossal dielectric constant in Nd1− xSrxFeO3 (0.1≤ x≤ 0.5). Materials Research Bulletin, 60, 474-484.

Alaeddin, A. S., & Poopalan, P. (2010). Impedance/modulus analysis of sol–gel Ba_xSr_1-xTiO_3 thin films. J Korean Phys Soc, 57, 1449-1455.

Arora, M., Arora, V., Kaur, S., Kaur, J., Kumar, S., & Singh, A. (2023). Evidence of non-debye behavior of Pb0. 76Sm0. 24Ti0. 76Fe0. 24O3 ceramics by complex impedance spectroscopy. Materials Today: Proceedings, 80, 1079-1085.

Bashir, J., & Shaheen, R. (2011). Structural and complex AC impedance spectroscopic studies of A2CoNbO6 (A= Sr, Ba) ordered double perovskites. Solid state sciences, 13(5), 993-999.

Dabas, S., Kumar, M., & Thakur, O. P. (2020). Investigation on structural, magnetic, dielectric and impedance spectroscopy properties of 'Gd'modified multiferroic-ferroelectric solid solutions. Ceramics International, 46(11), 17361-17375.

Das, B. P., Choudhary, R. N. P., & Mahapatra, P. K. (2008). Impedance spectroscopy analysis of (Pb0. 93Gd0. 07)(Sn0. 45Ti0. 55) 0.9825O3 ferroelectrics. Indian Journal of engine and mater. science, 15, 152-156.

Deka, B., Ravi, S., & Pamu, D. (2017). Impedance spectroscopy and ac conductivity mechanism in Sm doped Yttrium Iron Garnet. Ceramics International, 43(13), 10468-10477.

Jonscher, A. K. (1977). The 'universal'dielectric response. nature, 267(5613), 673-679.

Mesrar, M., Elbasset, A., Echatoui, N. S., Abdi, F., & Lamcharfi, T. (2023). Microstructural and high-temperature dielectric, piezoelectric and complex impedance spectroscopic properties of K0. 5Bi0. 5TiO3 modified NBT-BT lead-free ferroelectric ceramics. Heliyon, 9(4).1-17.

Primo-Martin, V., & Jansen, M. (2001). Synthesis, structure, and physical properties of cobalt perovskites: Sr3CoSb2O9 and Sr2CoSbO6− δ. Journal of Solid State Chemistry, 157(1), 76-85.

Roy, A. K., Prasad, K., & Prasad, A. (2013). Piezoelectric, impedance, electric modulus and AC conductivity studies on (Bi0. 5Na0. 5) 0.95 Ba0. 05TiO3 ceramic. Processing and Application of Ceramics, 7(2), 81-91.

Siqueira, F. B. L. B., & Campos, D. C. (2023). Application of impedance spectroscopy to analyze the electrical properties of cobalt doped SrTiO3. Solid State Ionics, 391, 116140.

Thakur, S., Rai, R., Bdikin, I., & Valente, M. A. (2016). Impedance and modulus spectroscopy characterization of Tb modified Bi 0.8 A 0.1 Pb 0.1 Fe 0.9 Ti 0.1 O 3 ceramics. Materials Research, 19, 1-8.